When and Where Lithium Plating Occurs, Its Correlation with Microstructure Heterogeneity, and the Mechanisms That Initiate and Self-Regulate Electrochemical Heterogeneity (A02-0444)

Francois L. E. Usseglio-Viretta[1], Andrew M. Colclasure[1], Jeffery M. Allen[2], Donal P. Finegan[1], Peter Graf[2], and Kandler Smith[1]

1. Center for Energy Conversion & Storage Systems, National Renewable Energy Laboratory, Golden, Colorado 80401, USA
2. Computational Science Center, National Renewable Energy Laboratory, Golden, Colorado 80401, USA

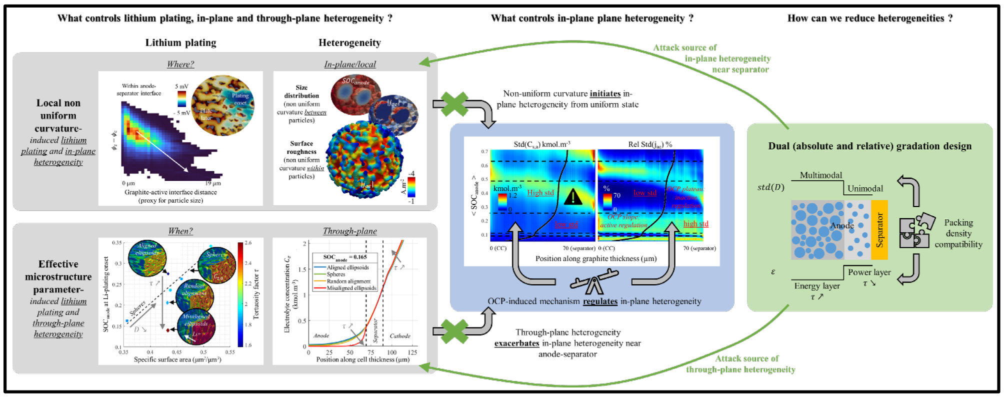

Non-uniform material utilization is detrimental to battery life and can cause earlier degradations (e.g., Lithium plating)

- Effective microstructure parameters, tortuosity factor and particle size/specific surface area, control through-plane heterogeneities and average onset of lithium plating (***when***).
- Non-uniform curvature, that is particle size distribution (between particle heterogeneity) and surface roughness (within particle heterogeneity), initiates in-plane/local heterogeneities and controls local onset of lithium plating (***where***).
- An **OCP-induced mechanism regulates** state of charge in-plane heterogeneity and prevents a snowball effect.
- Proposed **dual (uniformity and porosity) gradation anode design** to reduce, respectively, source of in-plane heterogeneity and source of through-plane heterogeneity.

Battery microstructure-scale electrochemical model

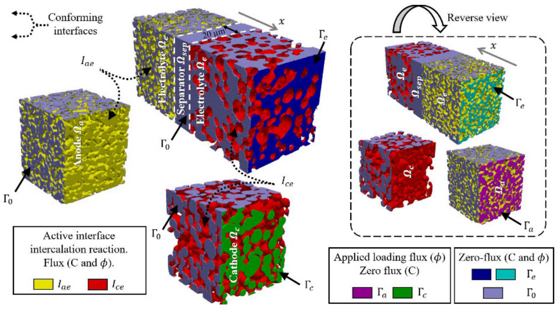

Type	DOF	Location	Boundary condition
Applied loading	Potential flux	Γ_a	$j_a \cdot \boldsymbol{n} = g_a$
		Γ_c	$j_c \cdot \boldsymbol{n} = g_c$
	with	$\begin{cases} G\,[A] = \dfrac{V_{\Omega_c}\,[m^3] \times C_{s\,max,c}[mol.m^{-3}] \times SOC_{range,c}\,[\,] \times C_{th}\,[\,] \times F[As.mol^{-1}]}{3600[s]} \\ g_a = G/S_{\Gamma_a} \\ g_c = G/S_{\Gamma_c} \end{cases}$	
Intercalation reaction	Potential flux	I_{ae}	$j_a \cdot \boldsymbol{n} = j_e \cdot \boldsymbol{n} = j_{ae}$
		I_{ce}	$j_c \cdot \boldsymbol{n} = j_e \cdot \boldsymbol{n} = j_{ce}$
	Concentration flux	I_{ae}	$N_a \cdot \boldsymbol{n} = N_e \cdot \boldsymbol{n} = \dfrac{j_{ae}}{F}$
		I_{ce}	$N_c \cdot \boldsymbol{n} = N_e \cdot \boldsymbol{n} = \dfrac{j_{ce}}{F}$
	with	$\begin{cases} \text{Faraday current density} & j_{me} = i_{0,m}\left(e^{\frac{F}{2RT}\eta_m} - e^{\frac{-F}{2RT}\eta_m}\right) = 2i_{0,m}\sinh\left(\frac{F}{2RT}\eta_m\right) \\ \text{overpotential} & \eta_m = \phi_{s,m} - \phi_e - U_m \end{cases}$	
Balance between applied loading and intercalation reaction	(implicit) $G = \iint_{\Gamma_a} g_a\,dS = \iint_{I_{ae}} j_{ae}\,(S_{r,a} \times dS) = \iint_{I_{ce}} j_{ce}\,(S_{r,c} \times dS) = \iint_{\Gamma_c} g_c\,dS$		
Zero-flux	Potential flux	Γ_e	$j_e \cdot \boldsymbol{n} = 0$
	Concentration flux	Γ_a	$j_a \cdot \boldsymbol{n} = 0$
		Γ_c	$j_s \cdot \boldsymbol{n} = 0$
Zero-flux (symmetry condition)	Potential flux	Γ_0	$j_a \cdot \boldsymbol{n} = j_c \cdot \boldsymbol{n} = j_e \cdot \boldsymbol{n} = 0$
	Concentration flux	Γ_0	$N_a \cdot \boldsymbol{n} = N_c \cdot \boldsymbol{n} = N_e \cdot \boldsymbol{n} = 0$

Domain	DOF	Conservation equations	Flux equations
Solid $\Omega_a \cup \Omega_c$	Species	$\dfrac{\partial C_{s,m}}{\partial t} = -\nabla \cdot N_m$	$N_m = -D_{s,m}\nabla C_{s,m}$
	Charge	$0 = -\nabla \cdot j_m$	$j_m = -\kappa_{s,m}\nabla\phi_{s,m}$
Electrolyte $\Omega_{sep} \cup \Omega_e$	Species	$\dfrac{\partial(\varepsilon_{pore}^{nano} C_e)}{\partial t} = -\nabla \cdot N_e$ $\varepsilon_{pore}^{nano} = \begin{cases} 1 - \varepsilon_{sep} \text{ as } \varepsilon_{pore}^{nano} + \varepsilon_{sep} = 1 & \text{if } x \in \Omega_{sep} \\ 1 - \dfrac{\varepsilon_{CBD}}{1 - \varepsilon_{AM}} & \text{if } x \in \Omega_e \\ \text{as } \varepsilon_{pore}^{nano}\varepsilon_{[pore+CBD]} + \varepsilon_{AM} + \varepsilon_{CBD} = 1 & \end{cases}$	$N_e = -D_e^{micro}\nabla C_e + \dfrac{t_0^+}{F} j_e$ with $\dfrac{D_e^{micro}}{D_e^{bulk}} = \dfrac{\varepsilon_{pore}^{nano}}{\tau^{nano}}$
	Charge	$0 = -\nabla \cdot j_e$	$j_e = -K_e^{micro}\nabla\phi_e - K_D^{*}\nabla C_e$ with $\dfrac{K_e^{micro}}{K_e^{bulk}} = \dfrac{\varepsilon_{pore}^{nano}}{\tau^{nano}}$ $K_D = K_e^{micro}(t_0^+ - 1)(1 + A_c)\dfrac{2RT}{F}$ $K_D^{*} = K_D/C_e$

- (top left): boundary locations and domains visualized on a full-cell microstructure mesh (current collectors are not represented).
- (top right): Boundary conditions at the interfaces
- (bottom right): Conservation and flux equations in the volumes

Volumes and interfaces are noted, respectively, Ω

*Volumes and interfaces are noted, respectively, Ω_* and Γ_* with the subscript * being the material or interface domain (a = anode, c = cathode, e = electrolyte, sep = separator).*
Superscript micro indicates the electrolyte diffusivity and conductivity coefficients are homogenized from nanoscale. Superscript nano for the electrolyte porosity term correspond to the porosity of the homogenized phase.

J. M. Allen, J. Chang, F. L. E. Usseglio-Viretta, P. Graf, and K. Smith, *A Segregated Approach for Modeling the Electrochemistry in the 3-D Microstructure of Li-Ion Batteries and Its Acceleration Using Block Preconditioners*, Journal of Scientific Computing , 2021

Microstructure geometries

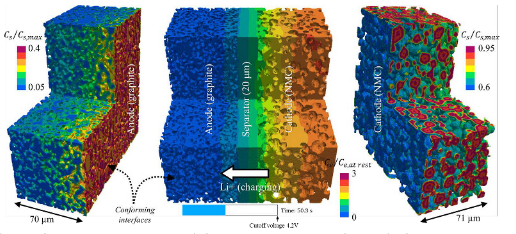

(**X-ray Computed Tomography**) Concentration solution fields of XCEL round 2 cell (NMC532/Gr) during 6C charge (34M Degrees of freedom).

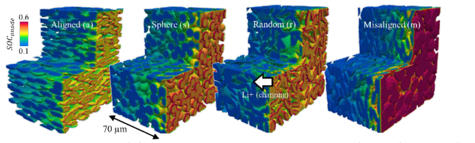

(**Numerically generated**) Solid concentration snapshot at 60s for a 6C charge for the 4 graphite geometries

Microstructure meshing (Iso2mesh, Q. Fang, 2009) and virtual microstructure generation performed with NREL open-source microstructure analysis toolbox (MATBOX)

F. L. E. Usseglio-Viretta, P. patel, E. Bernhardt, A. Mistry, P. P. Mukherjee, J. Allen, S. J. Cooper, J. Laurencin, and K. Smith, *MATBOX: An Open-source Microstructure Analysis Toolbox for microstructure generation, segmentation, characterization, visualization, correlation, and meshing*, SoftwareX, 2022

Heterogeneity quantification

Through-plane

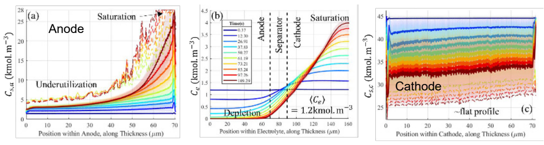

@6C
- Anode saturation
- electrolyte depletion

Controlled by tortuosity factor τ

$\dfrac{D_{eff}}{D_{bulk}} = \dfrac{\varepsilon}{\tau} = \varepsilon^p$

Variable C-rate
- Increasing in-plane heterogeneity
- **Dynamic through-plane intercalation rate profile**, with a propagation front from the anode-separator interface to the back of the electrode

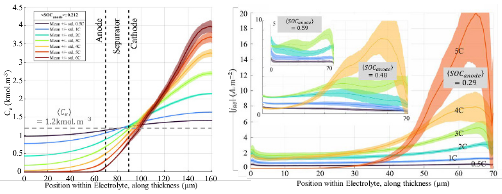

In-plane

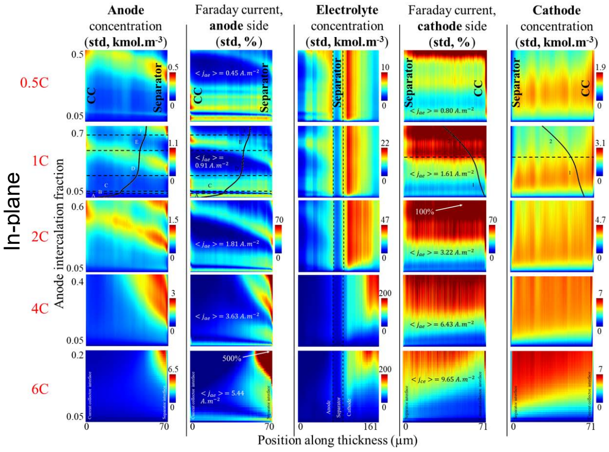

In-plane standard deviation

Std(C$_e$): up to 100 mol.m^{-3} at the separator interface and **up to ~200 mol.m^{-3}** (~16% of at rest Ce) at the current collector interface. Separator significantly suppresses the in-plane heterogeneity electrolyte concentration

Std(C$_s$): **up to 6-7 kmol.m^{-3}** in both electrodes at fast charge, near the separator interface for the anode, and in large part of the electrode volume for the cathode

Std(j): >100% for the anode near the separator interface.

In-plane heterogeneity propagation front within the anode, from the separator interface to the back of the electrode.

In-plane heterogeneity sources

Non-uniform curvature

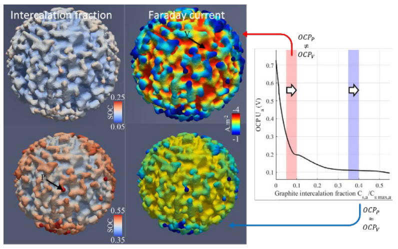

6C lithiation of a numerically generated single graphite spherical particle of diameter 10 µm with submicron surface roughness. Images show calculated results after a volume-averaged SOC increase of 0.05 from different starting SOC.

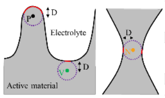

	Active material concentration	Overpotential (OCP)	Faraday current density
Curvature	+		
Active material concentration		+ if not in an OCP plateau and/or at high charge rate	
Overpotential			+
Faraday current density	-		

Read as follow: curvature in-plane heterogeneity induces active material concentration in-plane heterogeneity

Non-uniform diameter

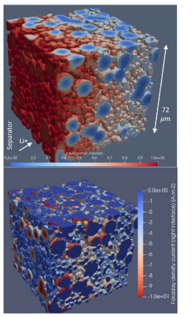

6C lithiation of a numerically generated half-cell graphite with bimodal spherical particle (without surface roughness).

Lithium-plating in-plane heterogeneity and correlation with microstructure

Potential for lithium plating at the anode-separator interface$\phi_s - \phi_e$

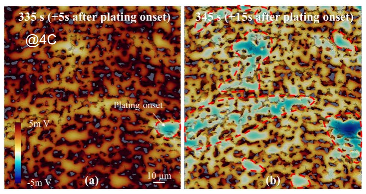

Model predicts **non-uniform lithium plating even for small regions (154 x 144 µm^2).** It takes ~32s @4C to reach the plating condition within the full interface.

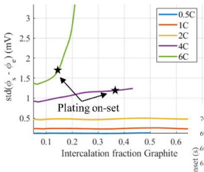

The higher the C-rate, the higher the plating heterogeneity

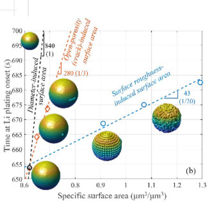

Interface-bulk distance (~ particle diameter), and not specific surface area, **controls the plating onset** (with tortuosity)

F. L. E. Usseglio-Viretta, A. M. Colclasure, J. M. Allen, D. P. Finegan, P. Graf, and K. Smith, Microstructure Scale Lithium-ion Battery Modeling, Part I: on lithium plating prediction and heterogeneity, In redaction

This work was authored by the National Renewable Energy Laboratory, operated by Alliance for Sustainable Energy, LLC, for the U.S. Department of Energy (DOE) under Contract No. DE-AC36-08GO28308. Funding provided by the U.S. Department of Energy Office of Energy Efficiency and Renewable Energy, Vehicle Technology Office, eXtreme Fast Charge and Cell Evaluation of Lithium-Ion Batteries (XCEL) Program, program manager Samuel Gillard. This research was performed using computational resources sponsored by the U.S. Department of Energy's Office of Energy Efficiency and Renewable Energy and located at the National Renewable Energy Laboratory. The views expressed in the article do not necessarily represent the views of the DOE or the U.S. Government. The U.S. Government retains and the publisher, by accepting the article for publication, acknowledges that the U.S. Government retains a nonexclusive, paid-up, irrevocable, worldwide license to publish or reproduce the published form of this work, or allow others to do so, for U.S. Government purposes.

245th Electrochemical Society Meeting
Marriott Marquis – San Francisco, California
May 26-30, 2024
NREL/PO-5700-89923